

Annual Review of Physical Chemistry

Multiconfiguration Pair-Density Functional Theory

Prachi Sharma,^{1,*} Jie J. Bao,^{1,*} Donald G. Truhlar,¹
and Laura Gagliardi²

¹Department of Chemistry, Chemical Theory Center, and Minnesota Supercomputing Institute, University of Minnesota, Minneapolis, Minnesota 55455, USA; email: truhlar@umn.edu

²Department of Chemistry, Pritzker School of Molecular Engineering, James Franck Institute, and Chicago Center for Theoretical Chemistry, The University of Chicago, Chicago, Illinois 60637, USA; email: lgagliardi@uchicago.edu

Annu. Rev. Phys. Chem. 2021. 72:541–64

The *Annual Review of Physical Chemistry* is online at
physchem.annualreviews.org

<https://doi.org/10.1146/annurev-physchem-090419-043839>

Copyright © 2021 by Annual Reviews.
All rights reserved

*These authors contributed equally to this article.

Keywords

correlation energy, density functional theory, multiconfigurational wave function, electronic structure theory, molecular energetics, quantum chemistry, spectroscopy

Abstract

Kohn-Sham density functional theory with the available exchange–correlation functionals is less accurate for strongly correlated systems, which require a multiconfigurational description as a zero-order function, than for weakly correlated systems, and available functionals of the spin densities do not accurately predict energies for many strongly correlated systems when one uses multiconfigurational wave functions with spin symmetry. Furthermore, adding a correlation functional to a multiconfigurational reference energy can lead to double counting of electron correlation. Multiconfiguration pair-density functional theory (MC-PDFT) overcomes both obstacles, the second by calculating the quantum mechanical part of the electronic energy entirely by a functional, and the first by using a functional of the total density and the on-top pair density rather than the spin densities. This allows one to calculate the energy of strongly correlated systems efficiently with a pair-density functional and a suitable multiconfigurational reference function. This article reviews MC-PDFT and related background information.

ANNUAL
REVIEWS **CONNECT**

www.annualreviews.org

- Download figures
- Navigate cited references
- Keyword search
- Explore related articles
- Share via email or social media

1. INTRODUCTION

Kohn-Sham (KS) theory (1, 2), spin-polarized KS theory (3–5), and generalized KS theory (6, 7) revolutionized the application of quantum mechanical electronic structure theory by enabling practical calculations of geometric structures, spectroscopic properties, thermodynamic quantities, and dynamics for large and complex systems (8). A KS calculation uses a single Slater determinant to represent the electronic density and optimizes the orbitals of that determinant to minimize an energy expression containing the kinetic energy of that determinant, its classical electrostatic energy, and a functional of the spin densities (α spin and β spin densities). The functional is technically called the exchange–correlation functional and is sometimes written as a sum of an exchange part and a correlation part; however, it is also often simply called the density functional. Although KS-DFT (density functional theory) is an exact theory in the sense that there is an existence theorem for an exchange–correlation functional that would yield the correct quantum mechanical density and energy, finding that exact functional is practically impossible; as a result, many approximate density functionals have been proposed and used for practical applications. The functionals may be classified in various ways, for example, as local spin density approximations (LSDAs), gradient approximations (GAs), meta-GAs, and hybrid functionals. For many properties, such as barrier heights of chemical reactions, KS theory with the currently available functionals is, on average, more accurate than many more-expensive wave function methods.

Although KS theory with approximate functionals has been very successful, it has two major shortcomings. One is the lower accuracy typically obtained for calculations on strongly correlated states, and the other is the so-called symmetry dilemma (9–11), which also affects Hartree-Fock theory.

A configuration state function (CSF) is an electronic eigenfunction corresponding to a particular way to assign electrons to orbitals (2, 1, or 0 electrons in each orbital); it is also a spin eigenfunction, that is, an eigenfunction of S^2 and S_z , where S is total electron spin and S_z is a component of the spin angular momentum. Strongly correlated states are those for which a single CSF does not provide a good zero-order reference state; in other words, strongly correlated states are states that are inherently multiconfigurational. In wave function theory (WFT), the most efficient way to describe strongly correlated states is to use a multiconfigurational reference function; hence, such states are often called multireference (MR) states.

A manifestation of the symmetry dilemma is that one can sometimes find a Slater determinant (which is the simplest single-configuration wave function) that gives a good zero-order estimate of the energy only if the determinant is not a spin eigenfunction; this is the case, for example, for biradicals such as those obtained when one homolytically stretches a covalent bond to a large internuclear distance. In such a case, a Slater determinant that is restricted to being a spin eigenfunction provides a poor description of the energy. If one wants to emphasize the spin-eigenfunction restriction, a KS calculation with a Slater determinant restricted to being a spin eigenfunction is called restricted KS (RKS) for closed-shell singlets and restricted open-shell KS (ROKS) for open shells; the restriction is enforced by requiring the α spin and β spin electrons of doubly occupied orbitals to be in identical spatial orbitals. Because KS theory satisfies a variational principle, one should find the variationally best solution by allowing different orbitals for α spin and β spin electrons; doing this yields a Slater determinant that is not a spin eigenfunction if the variationally best solution has different orbitals for different spins (DODS). If one wants to emphasize that a KS calculation uses DODS, one may call it a spin-polarized or unrestricted KS (UKS) calculation.

The symmetry dilemma of KS-DFT is illustrated in **Figure 1** for the ground-state dissociation of the H–H bond in the H_2 molecule. The figure presents the RKS and UKS potential energy curves and the UKS value of $\langle S^2 \rangle$, which is 0 for a pure singlet state. The RKS calculation

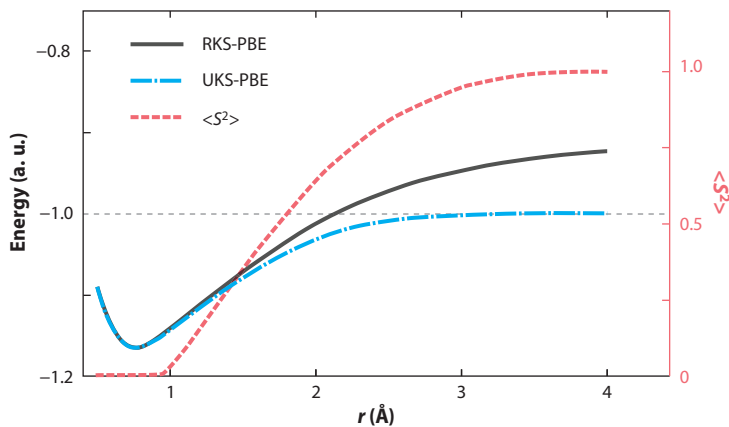


Figure 1

H_2 energy by RKS-PBE and UKS-PBE and the expectation value of S^2 by UKS-PBE. All calculations for this figure were carried out using *OpenMolcas* (12) with the PBE functional (13) and the jun-cc-pVTZ basis set (14). The abscissa is the H–H distance. The gray dashed line (-1 a. u.) indicates the correct energy at dissociation. The red dashed line indicates the expectation value of S^2 , which, for the ground state of H_2 , is zero when UKS-PBE preserves the spin symmetry or nonzero when UKS-PBE breaks the spin symmetry. Abbreviations: cc, correlation consistent; PBE, Perdew-Burke-Ernzerhof; pVTZ, polarized valence triple zeta; RKS, restricted Kohn-Sham; UKS, unrestricted Kohn-Sham.

preserves the spin symmetry for the ground state of H_2 , and this results in $\rho_\alpha = \rho_\beta = \frac{\rho}{2}$ (where ρ_α , ρ_β , and ρ are α spin density, β spin density, and electron density, respectively) throughout the dissociation. The UKS calculation, in contrast, allows for full relaxation of orbitals, and this results in the UKS Slater determinant not having singlet spin symmetry at large internuclear distances. As a result, UKS preserves the spin symmetry only for internuclear distances near the equilibrium one, and it becomes RKS and quickly breaks the symmetry after 1 \AA , as shown in **Figure 1**. This means that the UKS determinant does not have $\rho_\alpha = \rho_\beta = \frac{\rho}{2}$, although this holds for the exact wave function. The spin densities are not necessarily exact (i.e., they are not necessarily the same as for a solution to the Schrödinger equation), even with the unknown exact exchange-correlation functional, although their sum (the electron density) would be exact with that functional. Thus, even if one could use the unknown exact functional that yields the correct energy, the Slater determinant would not necessarily be a spin eigenfunction, because S^2 is a many-electron operator (it is a two-electron operator for H_2). KS theory with the unknown exact functional gives the exact electron density and the exact energy, but not only does it not necessarily give the exact spin densities, it also does not necessarily give the exact spinless one-electron density matrix (2), nor—with the exception of the energy—does it generally give the exact value of properties that depend on the two-electron density matrix.

The RKS solution for H_2 at long distances corresponds to 50% $\text{H} \dots \text{H}$, 25% $\text{H}^+ \dots \text{H}^-$, and 25% $\text{H}^- \dots \text{H}^+$ rather than the correct 100% $\text{H} \dots \text{H}$; this yields a very high energy. In contrast, the UKS broken-symmetry energy in **Figure 1** quickly approaches -1 hartree (which is the exact energy of two infinitely separated H atoms), and the Slater determinant tends to 100% $\text{H} \dots \text{H}$. However, the UKS Slater determinant dissociates to a wave function with all of the α spin on one atom and all of the β spin on the other. A singlet spin eigenfunction has $\rho_\alpha = \rho_\beta$ at all points in space, resulting in each atom having 50% α spin and 50% β spin. Coulson & Fischer (15) showed that one can find a two-configuration wave function that not only has $\rho_\alpha = \rho_\beta$ at all points in space but also dissociates to 100% $\text{H} \dots \text{H}$. However, if we were to calculate the dissociation energy with

approximate KS functionals using these singlet spin densities that have $\rho_\alpha = \rho_\beta$, we would get a poor result (more than 50 kcal/mol too high) because customary KS functionals give a good answer for an H atom with 100% α spin or β spin but an unsatisfactory one for an H atom with 50% α spin and 50% β spin.

Therefore, we cannot remedy the symmetry dilemma of KS-DFT by simply applying available KS density functionals to a multiconfigurational wave function that provides a good zero-order reference function. However, as already illustrated for H_2 , useful results can be obtained in many cases by calculating energies using the variationally optimized broken-symmetry UKS Slater determinants even though they have the incorrect spin symmetry (16–22). Although the discussion in this section has used H_2 calculations with the Perdew–Burke–Ernzerhof (PBE) functional for illustration, the issue is more pervasive, and the discussion is applicable to many open-shell calculations with all KS functionals in common use.

Yu et al. (23) summarize the performance of a variety of KS density functionals (without symmetry restrictions) on SR (single-reference) and MR systems. Although the best functional included in the study can reduce the mean unsigned error (MUE) for 54 MR systems to 4.35 kcal/mol, this error is still twice as large as those reported for the 313 SR systems; for other functionals, the MUE for the MR systems can be three times as large as those for the SR systems. This is an indication that KS-DFT cannot describe MR systems as well as it describes SR systems. MR character “is not a rare phenomenon and . . . is generally unavoidable when considering the entire potential energy surface” (24, p. 189). It is particularly important for open-shell systems, stretched bonds, and excited states. The UKS approach is nevertheless widely used, often with good results. Sometimes ad hoc procedures are used to correct the spin symmetry, especially when the Slater determinant is very far from being a spin eigenfunction. Because one would get the accurate energy without such corrections if one had the unknowable exact KS functional, such corrections would move the result away from the correct energy. However, presently available functionals are far enough from the exact one that although the corrections do not always improve the accuracy (22), they sometimes do.

In WFT, by which we refer to methods that calculate the energy from an approximate or accurate solution to the Schrödinger equation without using a functional of the density, a single-Slater-determinant self-consistent field calculation is referred to as a Hartree–Fock calculation. The relatively poor performance of single-Slater-determinant KS theory for strongly correlated states has an analog in WFT in the relatively poor performance of calculations that use Hartree–Fock wave functions as reference states for subsequent calculations on strongly correlated systems. For example, coupled cluster calculations with single, double, and triple excitations from a Hartree–Fock reference state are usually reliable for weakly correlated systems but are less reliable for strongly correlated systems. This has motivated the development of a variety of MR wave function methods, which use multiconfigurational wave functions (a linear combination of Slater determinants or CSFs) as reference states (25–43). The most affordable MR methods in widespread use are based on perturbation theory, and they include both state-specific methods, such as complete active space (CAS) second-order perturbation theory (CASPT2) (28, 29) and n -electron valence state perturbation theory (NEVPT2) (38), and multistate methods, such as extended multistate CASPT2 (XMS-CASPT2) (39, 40), quasidegenerate NEVPT2 (41), and extended multiconfigurational quasidegenerate perturbation theory (33, 42). The multiconfigurational reference states are usually obtained by multiconfigurational self-consistent field (MCSCF) calculations, which include CAS self-consistent field (CASSCF) theory (44–47) [also called FORS (48)], restricted active space (RAS) self-consistent field (RASSCF) theory (49), generalized active space (GAS) self-consistent field (GASSCF) theory (50), and generalized valence bond (GVB) theory (51). CASSCF is an MCSCF method that corresponds to complete configuration interaction

(CCI) in an active space, meaning that one includes all CSFs that can be formed with a given spin symmetry for a given number of active electrons distributed in a given number of active orbitals; in contrast, RASSCF and GASSCF are MCSCF methods that include only a subset of those CSFs. [One can also use other kinds of multiconfigurational functions as references, for example, RAS configuration interaction (CI) (RASCI) (52), floating occupation molecular orbital–CASCI (53), CI singles natural orbitals CASCI (54), and pair-coupled cluster doubles (p-CCD) (55), but because MCSCF is a much more common choice, we continue our discussion in terms of MCSCF.] To obtain quantitatively accurate results at the MCSCF level, one would usually need to include more CSFs than are affordable in an MCSCF calculation. The calculation then proceeds by calculating the MCSCF energy and adding additional correlation energy by a post-SCF procedure (i.e., without further optimization of the orbitals). However, post-MCSCF correlation calculations with good accuracy tend to be very expensive, often impractically so, and this has motivated the development of multiconfigurational density functional methods.

A common way of discussing results in WFT is to divide correlation energy into static and dynamic correlation energy. The border between these is fuzzy, but one way to explain the distinction is to first define static correlation error. Static correlation error is the error attributable to using an approximate wave function that is not a useful zero-order wave function because it does not include enough nearly degenerate CSFs. For example, one cannot get a qualitatively correct wave function for the bond dissociation of H_2 with a single CSF, because a CSF is a spin eigenfunction; a single configuration that is a spin eigenfunction gives much too high an energy, and the error may be called static correlation error. As seen in the discussion of **Figure 1**, in KS theory this can be accounted for in some cases by breaking spin symmetry, in other words, by relaxing the requirement that the approximate wave function be a spin eigenfunction. But broken-symmetry solutions are unsatisfactory in other ways, one of which is that it is sometimes not clear whether one is actually approximating the state of interest rather than some state with another spin or some linear combination of states with different spins.

An MCSCF wave function can eliminate static correlation error without breaking spin symmetry; for example, by employing two CSFs one can eliminate the error in the description of H_2 at the dissociation asymptote, where the correction to the restricted Hartree-Fock result is called static correlation error. Dynamic correlation energy is the total correlation energy (which is defined as the difference between the exact energy and the Hartree-Fock energy) minus the static correlation energy. For an MCSCF calculation to provide a good reference function, it should include enough configurations to capture the static correlation energy. Inevitably then, it also recovers some dynamic correlation energy. We can illustrate this by considering H_2 at its equilibrium internuclear distance. There is only one low-energy CSF for this geometry, so there is no static correlation error and no static correlation energy. Thus, the energy difference between the two-CSF energy and the Hartree-Fock energy is purely dynamic correlation energy at this geometry, although two configurations are not enough to converge the dynamic correlation energy.

A useful way to discuss correlation energy in the context of MCSCF and post-MCSCF calculations is to divide correlation energy into internal and external components. Internal correlation energy is the energy included in the MCSCF calculation, and external correlation energy is the rest of the correlation energy. The previous paragraph illustrated how internal correlation energy may be static or dynamic or a combination of the two. For a general MR system, the MCSCF energy has both static and dynamic contributions, but including enough configurations in an MCSCF calculation to converge the correlation energy is impractical. Therefore, for quantitatively accurate results, the MCSCF wave function is used as a reference function for a subsequent post-SCF calculation, such as XMS-CASPT2 or XMC-QDPT (extended multiconfigurational quasidenerate perturbation theory). It could also be a reference for a larger CI calculation or for a

coupled-cluster-like calculation. This review is about using the MCSCF wave function as a reference function for a subsequent post-SCF pair-density functional calculation. Note that when we talk about functionals of the pair density, they are always also functionals of the total electron density.

Many density functional methods that attempt to add external correlation energy to the MCSCF energy have been proposed; however, there are two prominent problems. First, as already mentioned, KS density functionals do not usually give good results for MR systems when used with spin densities obtained from wave functions (such as MCSCF wave functions) that are spin eigenfunctions. Second, even when KS functionals do yield realistic energies with an MCSCF wave function, it is difficult to find a correlation functional that captures just the right amount of correlation, which is the amount not already included in the MCSCF energy (56).

An approach that avoids both of these problems is multiconfiguration pair-density functional theory (MC-PDFT) (57, 58), which combines a functional of the pair density with an MCSCF wave function that is a spin eigenfunction in a way that gives good results for an MR system. This review covers this theory and the applications of MC-PDFT, and it also briefly discusses some related work. One key aspect of MC-PDFT is that it does not use the internal correlation energy as a component of the final energy calculation. Another key aspect of this theory is that it uses on-top pair density (in addition to the total electron density used in KS theory). In the following sections, we define both the pair density and the on-top pair density and briefly discuss other density functional methods that also use the on-top pair density.

A density functional that uses the total density and on-top pair density as independent variables rather than the α and β spin densities is called an on-top functional, and the energy calculated from the on-top functional is called the on-top energy. Using such functionals may be considered an alternative to KS theory. However, theories employing the on-top functional from multiconfigurational reference states are not covered by the Hohenberg–Kohn theorem (59) that provides a rigorous starting point for KS theory.

The on-top pair density is the diagonal part of the reduced two-body density matrix in the coordinate representation, and it has been used in various density functional and density matrix functional contexts, with both Slater determinant reference states and multiconfigurational reference states. Reviewing all such work is beyond our scope; we concentrate on density functional methods that use the on-top pair density without using the rest of the two-body density matrix.

One final introductory point about static correlation energy is that local exchange functionals in KS theory automatically include some static correlation energy (60–62). Thus, a single Slater determinant need not be as poor in KS theory as in Hartree-Fock theory, and building better exchange-correlation functionals to treat strongly correlated systems with KS theory is an active area of research (63–67), although it is not included in the scope of this review.

2. INTRODUCTION TO PAIR-DENSITY FUNCTIONALS

Let x_i denote the spatial–spin coordinates r_i and σ_i of electron i . The pair density, also called the two-electron density, two-particle density, or reduced two-body density, of a system with N electrons is

$$P(r_1, r_2) = \frac{N(N-1)}{2} \int \Psi^*(x_1, x_2, \dots, x_N) \Psi(x_1, x_2, \dots, x_N) d\sigma_1 d\sigma_2 dx_3 \dots dx_N, \quad 1.$$

where Ψ is the electronic wave function. (Note that the integration over spins is a sum.) The pair density is the probability density of finding one electron at r_1 and another at r_2 . The on-top pair density is the probability of finding two electrons at a point r , and it is given by

$$\Pi(r) = P(r_1, r_2)|_{r_1=r_2=r}. \quad 2.$$

In KS-DFT, the exchange-correlation functional may be written either in terms of the α spin density, $\rho_\alpha(r)$, and the β spin density, $\rho_\beta(r)$, or in terms of the total density, $\rho(r)$, and the net spin density, $m(r)$, which is also called the spin polarization:

$$\rho(r) = N \int \Psi^*(x_1, x_2, \dots, x_N) \Psi(x_1, x_2, \dots, x_N) d\sigma_1 dx_2 \dots dx_N |_{r_1=r}, \quad 3.$$

$$\rho(r) = \rho_\alpha(r) + \rho_\beta(r), \text{ and} \quad 4.$$

$$m(r) = \rho_\alpha(r) - \rho_\beta(r). \quad 5.$$

For a single Slater determinant, one can show that

$$\Pi(r) = \rho_\alpha(r)\rho_\beta(r), \quad 6.$$

$$m(r) = \sqrt{[\rho(r)]^2 - 4\Pi(r)}, \quad 7.$$

$$\rho_{\alpha/\beta}(r) = \frac{1}{2} [\rho(r) \pm m(r)]. \quad 8.$$

Notice that for a closed-shell singlet, this gives

$$\Pi(r) = [\rho(r)/2]^2. \quad 9.$$

Moscardó & San-Fabián (68) proposed to derive broken-symmetry spin densities $\rho_{\alpha/\beta}(r)$ by using Equation 7 with Π obtained from a multiconfigurational wave function rather than a Slater determinant. These broken-symmetry spin densities were then used in LSDA correlation functionals to take advantage of the fact that available KS density functionals work well with broken-symmetry spin densities even when static correlation is important. Becke et al. (69) extended this idea to also convert LSDA exchange functionals to depend on ρ and Π .

Whereas the above-mentioned articles (68, 69) proposed ways to use the on-top pair density to calculate energies from multiconfigurational wave functions, other work (70, 71) used the on-top pair density in the context of KS theory. In particular, Colle & Salvetti (70) used the on-top pair density to derive a correlation functional for KS theory [this functional is the starting point for the widely used LYP (Lee-Yang-Parr) (72) correlation functional], and Perdew et al. (71) showed how a very similar framework could be used to eliminate the symmetry dilemma of spin-polarized KS calculations by reinterpreting the spin-polarized Slater determinant in terms of $\rho(r)$ and $\Pi(r)$ rather than $\rho_\alpha(r)$ and $m(r)$. Miehllich et al. (73) discussed this kind of treatment for MCSCF wave functions; they did not provide the equation they used for the energy, but apparently they were adding a density functional correlation energy to the CASSCF internal energy because the main problem they discussed was how to define the density functional so that it would “lead to vanishing DFT contributions in the limit of complete CI calculations” (73, p. 527). (CCI in a complete set of orbitals is equivalent to an exact solution of the Schrödinger equation.) Moscardó et al. (74) set the energy equal to the energy of an MCSCF wave function plus a density functional correlation contribution and wrote the latter in terms of the on-top pair density.

3. MULTIREFERENCE DENSITY FUNCTIONAL THEORY USING PAIR DENSITIES

3.1. Additive Multireference Density Functional Theory

Additive MR-DFT is defined here as a method that adds a density functional energy (usually an on-top energy) to an internal energy computed from a multiconfigurational state. Special cases

that have received the most attention are those in which the multiconfigurational wave function is obtained by CASSCF (56, 75–78) or by GVB (79, 80). “Central problems” of this kind of theory “concern the effective coupling between wave function and DFT method, the double counting of dynamical correlation effects, the choice of the proper input quantities for the DFT functional, the balanced treatment of core and active orbital correlation, of equal-spin and opposite-spin correlation effects, and the inclusion of spin polarization to handle closed- and open-shell systems in a balanced way” (56, p. 279). Some of these problems are alleviated by using the broken-symmetry spin densities already discussed, but the double counting of correlation energy in both WFT and DFT remains a serious problem (81).

Many approaches have been used to minimize the double-counting problem in additive methods (75, 78, 82–85). The most thorough attempt was by Gräfenstein & Cremer (56), who labeled the additive approach as CAS-DFT. They concluded, “This work has demonstrated that CAS-DFT cannot be set up as a simple combination of CASSCF and a DFT correlation functional” (56, p. 299). They managed to overcome many of the problems by using a method they called CAS-DFT2(CS,SPP,FOS,DS), which denotes “CAS-DFT using level 2 for the distinction of core and active orbital correlations, carried out with the Colle–Salvetti (CS) functional (70), using the Stoll–Pavlidou–Preuß (86) (SPP) functional for equal-spin correlation corrections, including spin polarization in the scaling procedure, and correcting with the Davidson–Staroverov (87) (DS) density for low-spin cases” (56, p. 279) and where FOS stands for factor for open-shell problems. A key aspect of their method is the attempt to eliminate the double counting of the correlation energy by scaling down the local correlation energy density in a position-dependent way, a procedure first introduced by Miehlich et al. (73). Gräfenstein & Cremer (56) did this in a density-dependent, orbital-dependent, spin-polarization-dependent way by using a parameterized scaling factor. But they also noted remaining problems that might require introducing a system-specific gap correction and other changes in the scaling and the treatment of the core. Despite the partial success of CAS-DFT2(CS,SPP,FOS,DS), the messages we take away from this very thorough analysis are that scaling would be the best way to make the additive method work, but a general scaling procedure would have to be very complicated and perhaps system-dependent, and it still might be unsatisfactory.

3.2. Constrained-Pairing Methods

Tsuchimochi & Scuseria (88) introduced a theory in which the wave function is a linear combination of determinants with different numbers of electrons, but the expectation value of the electron number operator over the wave function is correct, that is, the number of electrons is correct on average. This theory is called constrained-pairing mean-field theory (CPMFT) (88–91), and it attempts to describe static correlation at the cost of Hartree-Fock theory. Taking H_2 as an example (88), the CPMFT wave function is a linear combination of $|0\rangle$, $|\sigma_g\alpha\sigma_g\beta\rangle$, $|\sigma_u\alpha\sigma_u\beta\rangle$, and $|\sigma_g\alpha\sigma_g\beta\sigma_u\alpha\sigma_u\beta\rangle$, where σ_g and σ_u are molecular orbitals, $|0\rangle$ is a vacuum Slater determinant (no electrons), the next two determinants have two electrons each, and the last determinant contains four electrons.

Tsuchimochi & Scuseria (88) combined CPMFT with a KS correlation functional and broken-symmetry spin densities calculated from the on-top density of the CPMFT wave function. Using TPSS (Tao-Perdew-Staroverov-Scuseria) (92) for the KS correlation functional, they called the resulting theory CPMFT+ χ TPSSc (88). Scuseria and coworkers (89) later proposed the constrained-pairing generalized KS (CPGKS) method, which combines Hartree-Fock exchange with pair-density-based exchange and correlation; the functional is called an exchange-correlation-pair functional ($E_{\text{xc,p}}$).

3.3. Multiconfiguration Pair-Density Functional Theory

This section reviews MC-PDFT (57), the advantages of this theory, and its applications. This section also reviews methods based on MC-PDFT.

3.3.1. Formula. The equation for the energy in MC-PDFT is (57)

$$E^{\text{MC-PDFT}} = V_{\text{NN}} + T_e + V_{\text{Ne}} + V_{\text{ee}} + E_{\text{ot}}[\rho, \Pi], \quad 10.$$

where V_{NN} is the nuclear repulsion energy, T_e is the electron kinetic energy, V_{Ne} is the electron–nuclear attraction energy, V_{ee} is the classical electron–electron repulsion energy, and E_{ot} is the on-top energy. All of the terms except the last one are computed as in WFT from the MCSCF calculation, which includes the specification of the nuclear geometry that gives V_{NN} and is needed for V_{Ne} . Because V_{Ne} and V_{ee} (which together constitute the classical electronic Coulomb energy) can be computed from the electron density ρ , the only quantities taken from the electronic MCSCF calculations are T_e , ρ , and Π . Unlike the additive MR methods discussed in Section 2, MC-PDFT does not use the WFT calculation of the internal correlation energy. The motivation for this is to avoid double counting, which is discussed more fully next.

In additive MR–DFT approaches in which a density-functional correlation energy is added to an MCSCF energy, double counting of electron correlation arises. The MCSCF energy already includes some correlation energy, so one is including correlation in two different ways. There is no known way to make the two contributions to the correlation energy add up to the correct correlation energy. Therefore, one might be double counting some portion of the correlation energy by having it in both parts of the calculation. However, in MC-PDFT, the energy is the sum of three contributions: (a) an approximation of the kinetic energy that is computed from a multiconfigurational wave function, (b) an approximation of the classical Coulomb energy computed from the multiconfigurational wave function, and (c) the rest of the energy that is computed from an on-top energy computed in turn from the density and on-top pair density of the multiconfigurational wave function. Note that the classical Coulomb energy has no correlation energy (correlation energy, like exchange energy, is a quantal effect). Therefore, the correlation energy appears only in factor c . It is not included twice, so there is no double counting. Garza et al. (93) summarized this situation by saying that Equation 10 eliminates the double counting “exactly” (93, p. 3). Nevertheless, the total energy is not exact, because, just as in Kohn–Sham theory, we do not know an exact functional. (In fact, we do not have an existence theorem for an exact functional in MC-PDFT.)

Since its inception in 2014, MC-PDFT has been applied successfully to several physical and chemical properties (including binding energies, barrier heights, electronic excitation energies, and magnetic properties) of organic molecules and transition metal and main-group inorganic molecules. The biggest advantage of MC-PDFT is that it produces results comparable to those of the computationally expensive CASPT2 method at a fraction of the computational cost for the post-SCF step (94). The wall time for an MC-PDFT calculation of n molecules of H_2 with two active electrons in two active orbitals [denoted $(2n, 2n)$] is comparable to that of CASSCF, while a CASPT2 calculation becomes considerably more expensive for active spaces larger than $(12, 12)$ because a CASPT2 calculation requires more time and memory to transform integrals from the atomic orbital basis to the molecular orbital basis, to calculate three-body and four-body density matrices, and to solve the CASPT2 equations (94).

Another feature of MC-PDFT is the availability of analytical gradients for reference wave functions optimized with single-state or state-averaged (SA) CASSCF (95, 96). The analytic gradient enables one to obtain equilibrium geometries, transition-state geometries, trajectories for reaction dynamics, and many other molecular properties at a decreased computational cost compared to that of numerical gradients.

One of the limitations of MC-PDFT with a CASSCF reference state is the limited size of the active space that is affordable. However, PDFT can be used with any multiconfigurational reference state, and it requires only the kinetic energy, density, and on-top pair density. A PDFT calculation can be applied to systems that require big active spaces by using wave functions obtained by RASSCF, RASCI, or GASSCF theory. Furthermore, one can use the density matrix renormalization group (DMRG) (97–100) or variational two-body reduced density matrix (v2RDM) (101, 102) approximations to obtain the density matrices corresponding to CASSCF wave functions instead of calculating these wave functions with conventional full CI solvers. DMRG converges to CASSCF for sufficiently large bond dimensions M , but PDFT has been found to work well with DMRG wave functions even with small values of M (103).

3.3.2. On-top density functionals. The MC-PDFT method currently uses on-top functionals that are converted from existing local KS exchange-correlation functionals. As explained in Section 2, the conversion consists of using the electron density and the on-top pair density from a multiconfigurational calculation with proper spin symmetry to compute broken-symmetry spin densities that are then plugged into KS exchange-correlation functionals that work well with such broken-symmetry spin densities. We have defined two methods of doing this conversion: Translated functionals (57) do not include the gradient of the on-top pair density, while fully translated functionals (104) do include this gradient. The KS functionals that have been converted include an LSDA functional, GVWN3 (105, 106), and several generalized GA (GGA) functionals, such as Becke-LYP (BLYP) (106, 107), OreLYP (62, 108, 109), PBE (13), revPBE (110), and OPBE (13, 62). Translated KS functionals are indicated with the prefix “t,” for example, tOreLYP, and the fully translated ones have the prefix “ft,” for example, ftPBE.

Carlson et al. (111) compared the on-top density calculated by a CASSCF wave function for H_2 with two active electrons in two active orbitals [CAS(2,2)] at the equilibrium geometry and beyond the Coulson-Fischer (15) point, where the unrestricted Hartree-Fock wave function optimizes to the broken-symmetry solution. They found that the on-top density decreases rapidly to zero starting at the Coulson-Fischer point due to bond breaking. This shows that on-top densities can be used as an indicator of homolytic bond breaking when the active space contains the bonding and antibonding orbitals.

3.3.3. Pair-density functional theory for excited states. The MC-PDFT method can use an SA-CASSCF wave function (112) as well as a state-specific wave function, and this is very useful for calculating ground states and excited states in a balanced way. However, the MC-PDFT equation does not include the interactions between the reference states, and these must be included when states are nearly degenerate, such as in the vicinity of conical intersections, which are widespread (113) and important for photochemistry. Therefore, three methods have been proposed to include state interactions (SIs) in the PDFT calculations. These three methods are called SI-PDFT (114–116), extended multistate PDFT (XMS-PDFT) (117), and variational multistate PDFT (VMS-PDFT) (117). These methods are all based on setting up a model space of intermediate states in which the off-diagonal elements of the Hamiltonian are calculated by WFT and combined with MC-PDFT calculations of the diagonal elements. The methods differ in how the intermediate states are generated.

The SI-PDFT method generates the intermediate states in two steps. First, it projects a state-specific ground state into the space of SA states to generate a ground intermediate state. Then the other intermediate states are obtained by orthogonalization of the SA states. This worked well, but this procedure treats the ground state in an unbalanced way when compared to how it treats excited states. To avoid this imbalance, we proposed the XMS-PDFT and the VMS-PDFT methods.

The XMS-PDFT method uses the intermediate states in the XMS-CASPT2 (40) method, which is a modification of MS-CASPT2 (39), to satisfy the orbital invariance properties recommended by Granovsky (42). In MS-CASPT2 calculations, a Fock matrix of states is defined and used to generate the zero-order Hamiltonian and zero-order wave function. However, MS-CASPT2 ignores the off-diagonal elements in the Fock matrix, rendering it dependent on orbital rotations. Granovsky (42) suggested the use of a set of intermediate states that diagonalize the Fock matrix of states to remove the orbital-rotation dependence of MC-QDPT results, and he called the new method XMC-QDPT. The letter X in the acronym indicates that this method uses the intermediate states. Modifying MS-CASPT2 to use analogous intermediate states yields XMS-CASPT2 (40).

The VMS-PDFT method generates intermediate states by maximizing the sum of MC-PDFT energies for the intermediate states. Fourier analysis is used to accomplish this conveniently.

The XMS-PDFT method fails for some systems, but it is the most efficient among the three methods. VMS-PDFT has worked well in all cases tested, but it is the costliest. Although the SI-PDFT method requires less computational cost than does VMS-PDFT and is also found to work in all cases tested, it has the imbalance of treating both ground and excited states, and it uses two sets of orbitals, which makes it more difficult to calculate gradients. Recently, we have improved VMS-PDFT so it both is more efficient and works in cases in which XMS-PDFT fails. The resulting method is called compressed MS-PDFT (CMS-PDFT) (118).

3.3.4. Delocalization error and self-interaction error. Delocalization error and self-interaction error (SIE) are two issues that limit the accuracy of KS theory with currently available functionals.

Almost all KS-DFT functionals suffer from delocalization error (119, 120). Delocalization error leads to incorrect densities, thereby causing large errors in barrier heights, excitation energies, band gaps, and transition metal energetics. Because MC-PDFT uses physical electron densities derived from MCSCF, MC-PDFT is free from delocalization error (121).

Yang and coworkers (119) proposed a test based on the concept of fractional charge to isolate the delocalization energy by calculating the ionization potential (IP) of a well-separated cluster of He atoms. The atoms are placed at a distance such that the effective interaction energy between two atoms is zero. The calculated IP of the cluster should be the same as that for an individual He atom; however, this is not the case when delocalization error is present. When this test was carried out for MC-PDFT, cluster IP was found to be independent of the number of He atoms in the cluster (121).

SIE arises in KS-DFT because the exchange potential does not exactly cancel the self-interaction present in the classical Coulomb potential. There is no unique way to separate delocalization error and SIE in KS-DFT for multielectron systems, and therefore quantifying SIE is difficult (119, 122). Because MC-PDFT currently uses translated KS-DFT functionals, SIE is not completely eliminated, although the MCSCF densities are obtained without SIE.

Bao et al. (122) performed the following tests to check SIE in MC-PDFT: (a) the potential energy curves for dissociation of rare gas cation dimers, (b) the dissociation energies of dimeric radical cations, and (c) neutral reactions that are considered “extremely prone to the SIE” (122). They found that SIE is reduced by a factor of two or more in MC-PDFT as compared to KS-DFT. For problems such as $\text{ArKr}^+ \rightarrow \text{Ar} + \text{Kr}^+$, MC-PDFT gives potential curves qualitatively similar to those of the coupled cluster theory with single and double excitations and quasiperturbative triple excitations [CCSD(T)], which should be reasonably accurate for this problem, whereas KS-DFT curves have the wrong shape at large internuclear distances, which may be mainly attributed to SIE.

3.3.5. Active space selection. One of the issues faced by current MC-PDFT functionals is a failure to converge the energy upon increasing the number of CSFs in the active space (123). Although this is a formal deficiency, it has not been a serious problem in practice. In this regard, we note that in WFT, even when convergence properties are understood, they may have little relevance to practical concerns. For example, the possible convergence of perturbation theory as the order is increased does not guarantee the accuracy of this theory with affordable orders of perturbation (124), and the fact that CI calculations for a system with 100 electrons would formally converge if the excitation level were taken to centuples has little relevance to the accuracy when excitations are capped at doubles.

The nonsystematic selection of CSFs to include in the reference state is a serious problem with all MR methods in both WFT and DFT. We generally find that the results of MC-PDFT do not depend strongly on the choice of active space, provided that reasonable choices of active spaces are made. The question still arises, though, of how to make the theory systematic so it can be validated convincingly. This is one reason for our interest in the correlated participating orbitals (CPOs), the ABC and ABC2 schemes, and the separated pair approximation, as discussed next.

In modern work, the CSFs for a multiconfigurational reference state are almost always chosen by active space methods. There are three steps in specifying the CSFs in an active space method. In step 1, one decides which electrons are active; the rest of the electrons are inactive and are in the same set of doubly occupied orbitals in all CSFs. In step 2, one decides on a set of active orbitals; the CSFs are obtained by distributing the active electrons in the active orbitals. In step 3, one decides which CSFs to include. As mentioned in Section 1, in a CAS calculation, one includes all possible CSFs that can be made by distributing active electrons in active orbitals. In the RAS and GAS methods, one uses subsets of these CSFs; this pruning has been called the elimination of deadwood (125). For example, in GAS methods, the orbitals are divided into subspaces, and the user defines ranges for the number of electrons to be allowed in each subspace. The separated-pair (SP) approximation (126) is a special case of GASSCF in which each GAS subspace contains one to three electrons in (at most) two orbitals, and interspace excitations are not allowed. For example, the active space of a closed-shell wave function with $2m$ active electrons in $2m$ orbitals is partitioned into m subspaces in which each subspace contains two electrons in two orbitals. This substantially decreases the number of configuration space functions.

The CPO schemes are concerned with steps 1 and 2. Three CPO schemes have been defined (127, 128), namely nominal (nom), moderate (mod), and extended (ext). In nom, only the orbitals directly involved in the chemical process under study along with their correlating orbitals are used; in mod, additional bonding, antibonding, and nonbonding orbitals and their correlating orbitals are added to the nom active space, while ext consists of all the valence orbitals and their correlating orbitals. By using well-defined schemes for all three steps, one can remove the arbitrariness in CSF selection and thereby define a model chemistry in the sense defined by Pople (129).

So far, we have used one set of systematic schemes for ground states and another two for excited states, where different considerations must be taken into account. The CPO schemes and the SP approximation are for ground states. For excited states, we have developed the ABC (130) and ABC2 (131) schemes; these are ways to generate starting orbitals for SA-CASSCF and SA-RASSCF calculations and to specify the size of the active space.

In additive MR-DFT methods like CAS-DFT, one needs to use a density functional that depends on the active space choice, and considerable effort has gone into trying to scale the correlation energy in ways that depend on the active space. Because MC-PDFT does not suffer from double counting, we have only used on-top functionals that do not depend on the active space. If one wants to empirically optimize improved on-top functionals, though, it may be necessary to do so in the context of a well-defined scheme for active space selection.

3.4. λ Multiconfiguration Pair-Density Functional Theory

Garza et al. (93) proposed to use MC-PDFT with a p-CCD reference state; p-CCD can treat some strongly correlated systems well, and it has the advantage over CASSCF that its cost scales polynomially rather than exponentially with the size of the system. Garza and coworkers tested four related theories. MC-PDFT with a p-CCD reference state was called pCCD-0DFT; additive MR-DFT with density-dependent scaling (with the scale factor f) of an on-top correlation functional was called p-CCD+ f DFT; additive MR-DFT with an unscaled on-top correlation functional was called pCCD-1DFT. In the fourth method, called pCCD- λ DFT, the energy is a sum of three terms: the p-CCD energy computed with two-electron terms multiplied by λ , the on-top exchange energy multiplied by $1 - \lambda$, and the on-top correlation energy multiplied by $1 - \lambda^2$; they set $\lambda = 0.75$. The motivation for the latter three methods is that although the first method eliminates double counting exactly, it can bring in SIE due to the local nature of the on-top exchange functional. Therefore, the researchers sought a compromise between the SIE and the double-counting error. Note that pCCD- λ DFT reduces to pCCD-0DFT when $\lambda = 0$ and to pCCD-1DFT when $\lambda = 1$. Although the results of the methods were compared, drawing conclusions about the relative accuracy of MC-PDFT is difficult because MC-PDFT was employed only with translated LSDAs, whereas the other methods were employed with translated PBE functionals. However, the additive method without scaling, that is, pCCD-1DFT, suffers from overcounting correlation energy.

Mostafanejad & DePrince (132) applied MC-PDFT using a v2RDM method to obtain the required CASSCF density and on-top pair density; as mentioned in Section 3.3.1, this has the advantage of making calculations with larger active spaces more affordable. They also presented a method called λ MC-PDFT that is the same as pCCD- λ DFT except that p-CCD is replaced by CASSCF as the reference state (133). For $\lambda = 0$, this reduces to the original MC-PDFT. Making λ nonzero provides a potential way to improve the method.

3.5. Complete Active Space Π Density Functional Theory

Recently, Gritsenko, Pernal, and van Meer presented a new method called CAS Π DFT (134–137). This is an additive MR-DFT method with a scaled correlation energy, but it differs from other additive MR methods in two ways: (a) The scaling depends on the on-top density as well as the density, and (b) the scaled correlation functional is included during the orbital optimization (i.e., the scaled correlation functional is not added post-SCF). Although CAS Π DFT is successful in dissociating single-bonded molecules such as H₂, BH, and F₂, it misses out on the middle-range dynamic correlation of the same-spin electrons of the high-spin configurations. To account for this middle-range dynamic correlation, a correction term is added to CAS Π DFT, and the resulting theory is called CAS Π DFT+M.

CAS Π DFT has been successful in breaking multiple bonds and computing $\pi \rightarrow \pi^*$ excitations in small molecules. However, it is limited by the presence of empirical parameters that are not universally defined and that change from case to case (136).

4. AVAILABLE IMPLEMENTATIONS OF MULTICONFIGURATION PAIR-DENSITY FUNCTIONAL THEORY

MC-PDFT has been implemented in the following codes: *Molcas 8* (138), *OpenMolcas* (12), *PySCF* (139, 140), and *GAMESS* (141). DMRG can be used as the full CI solver when *OpenMolcas* is interfaced with *QC Maquis* (99, 100). *OpenMolcas* also has multistate PDFT options: SI-PDFT, XMS-PDFT, and VMS-DFT. Most of the applications described here were carried out with *Molcas 8* and *OpenMolcas*.

5. APPLICATIONS OF MULTICONFIGURATION PAIR-DENSITY FUNCTIONAL THEORY

In Section 3, we classified MR-DFT methods (excluding density matrix functional theory, which is not included in this review) into three classes: (a) MR additive methods, those that add a post-SCF correlation energy (typically derived from a KS correlation functional by scaling and conversion to broken-symmetry densities) to the internal energy of an MCSCF wave function computed by WFT; (b) MC-PDFT, in which the energy is computed using only the kinetic energy and density from a multiconfigurational wave function calculation plus an on-top density functional of the density and on-top pair density from the MCSCF calculation without using the MCSCF internal energy; and (c) CASPDFT, which does not fall cleanly into class *a* or *b*. In this section, we consider applications of MC-PDFT.

5.1. Bond Breaking and Binding Energies

The MC-PDFT method has been successfully applied to study the bond-breaking and binding energies of many organic and inorganic molecules (57, 94, 104, 126, 128, 142–148). The first paper on MC-PDFT included calculations of the dissociation energies of H_2 , N_2 , F_2 , Cr_2 , CaO , and NiCl (57); MC-PDFT (tPBE) was successful with an MUE of 0.3 eV as compared to 0.8 eV for CASSCF.

A recent application of MC-PDFT is the dissociation of alkaline earth dimers (145), which have small bond energies (as might be expected because the atoms have closed subshells). **Figure 2** shows dissociation curves for Mg_2 , for which the experimental dissociation energy is only 1.24 kcal/mol; MC-PDFT with the ftPBE functional is much more accurate than is KS-DFT with the PBE functional. When all the dimers from Be_2 to Ra_2 were considered with the ANO-RCC-VTZP (atomic natural-orbital relativistic core-correlated valence triple zeta with polarization) basis set, the MUE in bond energies (which range from 1 to 4 kcal/mol) and bond lengths of MC-PDFT are 0.6 kcal/mol and 0.02 Å, as compared to 1.7 kcal/mol and 0.4 Å for CASPT2 with the same reference states (149).

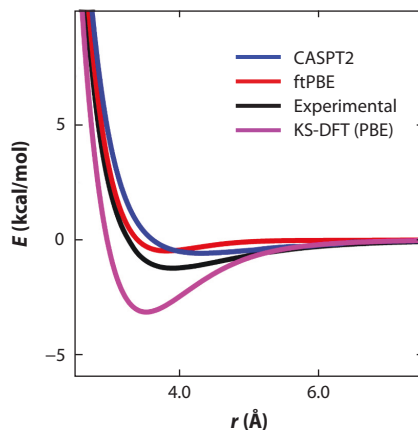


Figure 2

Dissociation curves for Mg_2 by CASPT2, ftPBE, and KS-DFT (PBE) using the ANO-RCC basis set. An active space of four electrons in eight orbitals consisting of all valence electrons is used. Abbreviations: ANO-RCC, atomic natural-orbital relativistic core-correlated; CASPT2, complete active space second-order perturbation theory; ftPBE, fully translated Perdew-Burke-Ernzerhof; KS-DFT, Kohn-Sham density functional theory. Figure adapted from Reference 145.

One of the strengths of MC-PDFT is that it recovers correlation energy well even for small active spaces such as those used in the SP approximation. Good results were obtained for binding energies of both main-group (126) and transition metal systems (143, 146) when SP-PDFT was used, where SP-PDFT denotes MC-PDFT with the SP scheme for CSF selection. Consider, for example, the results in Reference 143, which describes calculations employing the CPO selection scheme for the dissociation energies of 17 transition metal complexes with 2–5 atoms. The CASSCF reference states averaged 68,000 CSFs, whereas the SP reference states averaged 1,600 CSFs. The MUE in KS-DFT for these cases is 19 kcal/mol with the PBE functional and 16 kcal/mol with the BLYP functional, which provides another illustration of the inaccuracy of KS-DFT for strongly correlated systems. With the ftBLYP functional, however, PDFT has an MUE of only 6 kcal/mol with the CASSCF reference state and 5 kcal/mol with the smaller SP reference state.

In recent work, we (150) defined the extended SP (ESP) scheme in which all SP subspaces containing only one electron are merged into a bigger subspace; this was necessary to get good results for TiC and WCl. For TiSi, the experimental bond energy is 50.8 kcal/mol, and the translated revPBE functional (trevPBE functional) yields 50.1 kcal/mol with a CASSCF reference state (594 CSFs) and 51.9 kcal/mol with an ESP reference state (112 CSFs). With the same number of active electrons and active orbitals, CASSCF and CASPT2 give 22.0 and 48.3 kcal/mol, respectively.

Charge transfer complexes and their complexation energies have been extensively studied by KS-DFT, in which the quality of the results depends strongly on the choice of functional. The dissociation of energies of ground-state charge-transfer complexes was carried out using MC-PDFT for database CT7 (142, 151). Complexation energies calculated with tPBE have an MUE of 0.85 eV compared to 2.95 eV for KS-DFT with PBE; the comparable errors for CASSCF and CASPT2 are 3.92 and 1.66 eV, respectively (151).

Experimentally, the lowest-energy dissociation products of all diatomic molecules are neutral atoms, but this is not always the case in KS-DFT. For example, PBE with KS-DFT dissociates NaCl to Na⁺ and Cl⁻ ions, while MC-PDFT gives the right dissociation curve (148).

5.2. Barrier Heights

Barrier heights are important to predict the rate of a reaction as well as its probable reaction pathway, and MC-PDFT has been shown to provide good accuracy for transition-state energies (152). Recently, MC-PDFT analytical gradients were implemented, and this allows the efficient optimization of transition structures (95, 96). MC-PDFT was tested on the DBH24 database of barrier heights (153). One example is the reaction $\text{OH}^- + \text{CH}_3\text{F} \rightarrow \text{HOCH}_3 + \text{F}^-$, for which tPBE with MC-PDFT and a (4,4) active space predicts forward and reverse barrier heights to be -3.4 and 19.8 kcal/mol compared to the best estimate values of -2.7 and 17.6 kcal/mol, respectively.

5.3. Multiplet Splitting

MC-PDFT has been successful in predicting spin-state ordering and spin-state energy splittings (57, 103, 126, 128, 132, 154–158). Stoneburner et al. (156) calculated singlet-triplet splitting in diradical organic molecules and showed that MC-PDFT produces comparable results to CASPT2 even with small active spaces.

MC-PDFT has been applied to calculate spin-state ordering in several transition metal complexes (155, 157, 158). One such study includes the investigation of spin-state ordering in

nine Fe(II) and Fe(III) complexes with ligands of various strengths (155), in which MC-PDFT reproduces the results of CASPT2 at a lower cost. Iron porphyrin is one of the most challenging systems to which quantum mechanical methods have been applied; while CASPT2 and RASPT2 apparently give the wrong spin-ordering by predicting the quintet as being in the ground state instead of the triplet state, CAS-PDFT, RAS-PDFT, and DMRG-PDFT (depending on the active space size) calculate what is believed to be the correct spin-state ordering (158).

The singlet-triplet gaps in oligoacenes ranging from naphthalene to dodecacene were studied using v2RDM-PDFT and GAS-PDFT. These methods predicted adiabatic singlet-triplet gaps in polyacenes with an accuracy that is considerably higher than that of computationally more expensive methods such as CCSD(T) (103, 132, 154). These systems show the power of MC-PDFT for treating large systems. For example, a CASSCF calculation on a dodecacene triplet with all π electrons in the active space (50 active electrons in 50 active orbitals) would involve 10^{27} CSFs, but we got good results (mean accuracy for naphthalene through dodecacene of ~ 2 kcal/mol versus ~ 5 kcal/mol for GASSCF) with GAS-PDFT (with frontier partitioning) with 300,000 CSFs in the reference state (154). In another approach, we (103) used DMRG-PDFT to treat systems up to heptacene (30 active electrons in 30 active orbitals) within a CAS framework that does not require dividing the active space into further subspaces.

5.4. Other Excited States

MC-PDFT has been extensively applied to study other excited states of molecules containing main-group (57, 114–117, 147, 158–164, 165) and transition metal elements (104, 157, 158, 164, 166). For organic systems, excited-state calculations for a large data set containing valence, Rydberg, and charge transfer states show that MC-PDFT predicts excited-state energies and spectra as well as CASPT2, if not better (160). Another key feature of MC-PDFT is that it is stable with respect to the addition of diffuse basis functions, while methods such as time-dependent (TD)-KS-DFT suffer from an artificial lowering of the energies of high-energy states upon adding diffuse basis functions (164). Furthermore, MC-PDFT has been applied successfully to the calculation of vertical excitation energies for several challenging systems, including atoms; diatomic species such as cyano radicals (147); conjugated organic molecules such as butadiene (162), benzene (163), and retinal (161); conjugated and unconjugated cyclohexadienes (165) and 5,10-di(1-naphthyl)-5,10-dihydrophenazine (159); and transition metal complexes such as $\text{Re}_2\text{Cl}_8^{2-}$ (104), MnO_4^- (165), and iron porphyrin (158).

The SI-PDFT, XMS-PDFT, and VMS-PDFT multistate methods have been applied to study several challenging systems containing locally avoided crossings near conical interactions. These systems include LiF, phenol, methylamine, and mixed-valence strongly coupled states of the spiro molecule (114, 115, 117).

6. CONCLUDING REMARKS

MC-PDFT usually yields accuracy similar to or better than that of CASPT2 at a more affordable cost. It does not require system-specific scaling of density functionals or any other system-specific parameterization, which makes it a generally applicable first-principles technique. As methods for calculating multiconfigurational wave functions and/or density matrices become affordable for larger and more complex systems, MC-PDFT provides a practical way to calculate an energy with a treatment of the full correlation energy, even though the dynamic correlation energy computed from the multiconfigurational wave function by conventional wave function methods is far from convergence, as in most CASSCF calculations.

DISCLOSURE STATEMENT

The authors are not aware of any affiliations, memberships, funding, or financial holdings that might be perceived as affecting the objectivity of this review.

ACKNOWLEDGMENTS

The authors are grateful to Thais Scott for help with the manuscript. Our multiconfiguration pair-density functional theory research is supported in part by the National Science Foundation (grant CHE-1746186) and by the Air Force Office of Scientific Research (grant FA9550-16-1-0134).

LITERATURE CITED

1. Kohn W, Sham LJ. 1965. Self-consistent equations including exchange and correlation effects. *Phys. Rev.* 140:1133–38
2. Levy M. 1979. Universal variational functionals of electron densities, first-order density matrices, and natural spin-orbitals and solution of the v -representability problem. *PNAS* 76:6062–65
3. Stoddart JC, March NH. 1971. Density-functional theory of magnetic instabilities in metals. *Ann. Phys.* 64:174–210
4. von Barth U, Hedin L. 1972. A local exchange–correlation potential for the spin polarized case: I. *J. Phys. C Solid State Phys.* 5:1629–42
5. Rajagopal AK, Callaway J. 1973. Inhomogeneous electron gas. *Phys. Rev.* 87:1912–19
6. Becke AD. 1993. A new mixing of Hartree-Fock and local density-functional theories. *J. Chem. Phys.* 98:1372–77
7. Seidl A, Görling A, Vogl P, Majewski JA, Levy M. 1996. Generalized Kohn-Sham schemes and the band-gap problem. *Phys. Rev. B* 53:3764–74
8. Yu HS, Li SL, Truhlar DG. 2016. Perspective: Kohn-Sham density functional theory descending a staircase. *J. Chem. Phys.* 145:130901
9. Löwdin P-O. 1963. Discussion on the Hartree-Fock approximation. *Rev. Mod. Phys.* 35:496–501
10. Löwdin P-O. 1969. Some aspects of the correlation problem and possible extensions of the independent particle model. *Adv. Chem. Phys.* 14:283–340
11. Paldus J, Veillard A. 1978. Doublet stability of *ab initio* SCF solutions for the allyl radical. *Mol. Phys.* 35:445–59
12. Galván IF, Vacher M, Alavi A, Angeli C, Aquilante F, et al. 2019. OpenMolcas: from source code to insight. *J. Chem. Theory Comput.* 15:5925–64
13. Perdew JP, Burke K, Ernzerhof M. 1996. Generalized gradient approximation made simple. *Phys. Rev. Lett.* 77:3865–68
14. Papajak E, Zheng J, Xu X, Leverentz HR, Truhlar DG. 2011. Perspectives on basis sets beautiful: seasonal plantings of diffuse basis functions. *J. Chem. Theory Comput.* 7:3027–34
15. Coulson CA, Fischer I. 1949. Notes on the molecular orbital treatment of the hydrogen molecule. *Philos. Mag.* 40:386–93
16. Bagus PS, Bennet BI. 1975. Singlet-triplet splittings as obtained from the $X\alpha$ -scattered wave method: a theoretical analysis. *Int. J. Quantum Chem.* 9:143–48
17. Ziegler T, Rauk A, Baerends EJ. 1977. On the calculation of multiplet energies by the Hartree-Fock-Slater method. *Theor. Chim. Acta* 43:261–71
18. Noodleman L, Davidson ER. 1986. Ligand spin polarization and antiferromagnetic coupling in transition metal dimers. *Chem. Phys.* 109:131–43
19. Yamuguchi K, Tsunekawa T, Toyoda Y, Fueno T. 1988. Ab initio molecular orbital calculations of effective exchange integrals between transition metal ions. *Chem. Phys. Lett.* 143:371–76
20. Adamo C, Barone V, Bencini A, Broer R, Filatov M, et al. 2006. Comment on “About the calculation of exchange coupling constants using density-functional theory: The role of the self-interaction error” [J. Chem. Phys. 123, 164110 (2005)]. *J. Chem. Phys.* 124:107101

21. Cramer CJ, Truhlar DG. 2009. Density functional theory for transition metals and transition metal chemistry. *Phys. Chem. Chem. Phys.* 11:10757–816
22. Luo S, Averkiev B, Yang KR, Xu X, Truhlar DG. 2014. Density functional theory of open-shell systems. The 3D-series transition-metal atoms and their cations. *J. Chem. Theory Comput.* 10:102–21
23. Yu HS, He X, Li SL, Truhlar DG. 2016. MN15: a Kohn-Sham global-hybrid exchange-correlation density functional with broad accuracy for multi-reference and single-reference systems and noncovalent interactions. *Chem. Sci.* 7:5032–51
24. Lyakh DI, Musial M, Lotrich VF, Bartlett RJ. 2013. Multireference nature of chemistry: the coupled-cluster view. *Chem. Rev.* 112:182–243
25. Laidig WD, Saxe P, Bartlett RJ. 1987. The description of N₂ and F₂ potential energy surfaces using multireference coupled cluster theory. *J. Chem. Phys.* 86:887–907
26. Sun H, Freed KF. 1988. Molecular properties by *ab initio* quasidegenerate many-body perturbation theory effective Hamiltonian method: dipole and transition moments of CH and CH⁺. *J. Chem. Phys.* 88:2659–65
27. Illas F, Rubio J, Ricart JM. 1988. Approximate natural orbitals and the convergence of a second order multireference many-body perturbation theory (CIPSI) algorithm. *J. Chem. Phys.* 89:6376–84
28. Andersson K, Malmqvist PÅ, Roos BO, Sadlej AJ, Wolinski K. 1990. Second-order perturbation theory with a CASSCF reference function. *J. Phys. Chem.* 94:5483–88
29. Andersson K, Malmqvist P, Roos BO. 1992. Second-order perturbation theory with a complete active space self-consistent field reference function. *J. Chem. Phys.* 96:1218–26
30. Hirao K. 1992. Multireference Møller-Plesset method. *Chem. Phys. Lett.* 190:374–80
31. Nakano H. 1993. MCSCF reference quasidegenerate perturbation theory with Epstein-Nesbet partitioning. *Chem. Phys. Lett.* 207:372–78
32. Piecuch P, Oliphant N, Adamowicz L. 1993. A state-selective multi-reference coupled-cluster theory employing the single-reference formalism. *J. Chem. Phys.* 99:1875–900
33. Kozłowski PM, Davidson ER. 1994. Considerations in constructing a multireference second-order perturbation theory. *J. Chem. Phys.* 100:3672–82
34. Li X, Paldus J. 1998. Dissociation of N₂ triple bond: a reduced multireference CCSD study. *Chem. Phys. Lett.* 286:145–54
35. Finley J, Malmqvist PÅ, Roos BO, Serrano-Andrés L. 1998. The multi-state CASPT2 method. *Chem. Phys. Lett.* 288:299–306
36. Angeli C, Cimiraglia R, Evangelisti S, Leininger T, Malrieu JP. 2001. Introduction of *n*-electron valence states for multireference perturbation theory. *J. Chem. Phys.* 114:10252–64
37. Angeli C, Borini S, Cestari M, Cimiraglia R. 2004. A quasidegenerate formulation of the second order *n*-electron valence state perturbation theory approach. *J. Chem. Phys.* 121:4043–49
38. Angeli C, Pastore M, Cimiraglia R. 2007. New perspectives in multireference perturbation theory: the *n*-electron valence state approach. *Theor. Chem. Acc.* 117:743–54
39. Malmqvist PÅ, Pierloot K, Shahi ARM, Cramer CJ, Gagliardi L. 2008. The restricted active space followed by second-order perturbation theory method: theory and application to the study of CuO₂ and Cu₂O₂ systems. *J. Chem. Phys.* 128:204109
40. Mintz B, Williams TG, Howard L, Wilson AK. 2009. Computation of potential energy surfaces with the multireference correlation consistent composite approach. *J. Chem. Phys.* 130:234104
41. Shiozaki T, Győrffy W, Celani P, Werner HJ. 2011. Communication: Extended multi-state complete active space second-order perturbation theory: energy and nuclear gradients. *J. Chem. Phys.* 135:081106
42. Granovsky AA. 2011. Extended multi-configuration quasi-degenerate perturbation theory: the new approach to multi-state multi-reference perturbation theory. *J. Chem. Phys.* 134:214113
43. Yang KR, Jalan A, Green WH, Truhlar DG. 2013. Which *ab initio* wave function methods are adequate for quantitative calculations of the energies of biradicals? The performance of coupled-cluster and multi-reference methods along a single-bond dissociation coordinate. *J. Chem. Theory Comput.* 9:418–31
44. Roos BO, Taylor PR, Siegbahn PEM. 1980. A complete active space SCF method (CASSCF) using a density matrix formulated super-CI approach. *Chem. Phys.* 48:157–73
45. Roos BO. 1980. The complete active space SCF method in a Fock-matrix-based super-CI formulation. *Int. J. Quantum Chem.* 18:175–89

46. Siegbahn P, Heiberg A, Roos B, Levy B. 1980. A comparison of the super-CI and the Newton-Raphson scheme in the complete active space SCF method. *Phys. Scr.* 21:323–27
47. Siegbahn PEM, Almlöf J, Heiberg A, Roos BO. 1981. The complete active space SCF (CASSCF) method in a Newton–Raphson formulation with application to the HNO molecule. *J. Chem. Phys.* 74:2384–96
48. Ruedenberg K, Schmidt MW, Gilbert MM, Elbert ST. 1982. Are atoms intrinsic to molecular wave functions? I. The FORS model. *Chem. Phys.* 71:41–49
49. Malmqvist PÅ, Rendell A, Roos BO. 1990. The restricted active space self-consistent-field method, implemented with a split graph unitary group approach. *J. Phys. Chem.* 94:5477–82
50. Ma D, Li Manni G, Gagliardi L. 2011. The generalized active space concept in multiconfigurational self-consistent field methods. *J. Chem. Phys.* 135:044128
51. Hunt WJ, Hay PJ, Goddard WA III. 1972. Self-consistent procedures for generalized valence bond wavefunctions. Applications H₃, BH, H₂O, C₂H₆, and O₂. *J. Chem. Phys.* 57:738–48
52. Olsen J, Roos BO, Jørgensen P, Jensen HJA. 1988. Determinant-based configuration interaction algorithms for complete and restricted configuration interaction spaces. *J. Chem. Phys.* 89:2185–92
53. Slavíček P, Martínez TJ. 2010. *Ab initio* floating occupation molecular orbital-complete active space configuration interaction: an efficient approximation to CASSCF. *J. Chem. Phys.* 132:234102
54. Fales BS, Shu Y, Levine BG, Hohenstein EG. 2016. Complete active space configuration interaction from state-averaged configuration interaction singles natural orbitals: analytic first derivatives and derivative coupling vectors. *J. Chem. Phys.* 145:174110
55. Stein T, Henderson TM, Scuseria GE. 2014. Seniority zero pair coupled cluster doubles theory. *J. Chem. Phys.* 140:214113
56. Gräfenstein J, Cremer D. 2005. Development of a CAS-DFT method covering non-dynamical and dynamical electron correlation in a balanced way. *Mol. Phys.* 103:279–308
57. Li Manni G, Carlson RK, Luo S, Ma D, Olsen J, et al. 2014. Multiconfiguration pair-density functional theory. *J. Chem. Theory Comput.* 10:3669–80
58. Gagliardi L, Truhlar DG, Li Manni G, Carlson RK, Hoyer CE, Bao JL. 2017. Multiconfiguration pair-density functional theory: a new way to treat strongly correlated systems. *Acc. Chem. Res.* 50:66–73
59. Hohenberg P, Kohn W. 1964. Inhomogeneous electron gas. *Phys. Rev.* 136:B864–71
60. Cook M, Karplus M. 1987. Electron correlation and density-functional methods. *J. Phys. Chem.* 91:31–37
61. Tschinke V, Ziegler T. 1990. On the different representations of the hole-correlation functions in the Hartree-Fock and the Hartree-Fock-Slater methods and their influence on bond energy calculations. *J. Chem. Phys.* 93:8051–60
62. Handy NC, Cohen AJ. 2001. Left-right correlation energy. *Mol. Phys.* 99:403–12
63. Peverati R, Truhlar DG. 2014. The quest for a universal density functional: the accuracy of density functionals across a broad spectrum of databases in chemistry and physics. *Philos. Trans. R. Soc. A* 372:20120476
64. Dale SG, Johnson ER, Becke AD. 2017. Interrogating the Becke '05 density functional for non-locality information. *J. Chem. Phys.* 147:154103
65. Wang M, John D, Yu J, Proynov E, Liu F, et al. 2019. Performance of new density functionals of non-dynamic correlation on chemical properties. *J. Chem. Phys.* 150:204101
66. Verma P, Janesko BG, Wang Y, He X, Scalmani G, et al. 2019. M11plus: a range-separated hybrid meta functional with both local and rung-3.5 correlation terms and high across-the-board accuracy for chemical applications. *J. Chem. Theory Comput.* 15:4804–15
67. Verma P, Truhlar DG. 2020. Status and challenges of density functional theory. *Trends Chem.* 2:302–18
68. Moscardó F, San-Fabián E. 1991. Density-functional formalism and the two-body problem. *Phys. Rev. A* 22:1549–53
69. Becke AD, Savin A, Stoll H. 1995. Extension of the local-spin-density exchange-correlation approximation to multiplet states. *Theor. Chim. Acta* 91:147–56
70. Colle R, Salvetti O. 1979. Approximate calculation of the correlation energy for the closed and open shells. *Theor. Chim. Acta* 53:55–63

71. Perdew JP, Savin A, Burke K. 1995. Escaping the symmetry dilemma through a pair-density interpretation of spin-density functional theory. *Phys. Rev. A* 51:4531–41
72. Lee C, Yang W, Parr RG. 1988. Development of the Colle-Salvetti correlation-energy formula into a functional of the electron density. *Phys. Rev. B* 37:785–89
73. Miehlich B, Stoll H, Savin A. 1997. A correlation-energy density functional for multideterminantal wavefunctions. *Mol. Phys.* 93:527–36
74. Moscardó F, Muñoz-Fraile F, Pérez-Jiménez AJ, Pérez-Jordá JM, San-Fabián F. 1998. Improvement of multiconfigurational wave functions and energies by correlation energy functionals. *J. Phys. Chem. A* 102:10900–2
75. Malcolm NOJ, McDouall JJW. 1998. A simple scaling for combining multiconfigurational wavefunctions with density functionals. *Chem. Phys. Lett.* 282:121–27
76. Gräfenstein J, Cremer D. 2000. The combination of density functional theory with multi-configuration methods—CAS-DFT. *Chem. Phys. Lett.* 316:569–77
77. Gusarov S, Malmqvist PÅ, Lindh R. 2004. Using on-top pair density for construction of correlation functionals for multideterminant wave functions. *Mol. Phys.* 102:2207–16
78. Yamanaka S, Nakata K, Ukai T, Takada T, Yamaguchi K. 2006. Multireference density functional theory with orbital-dependent correlation corrections. *Int. J. Quantum Chem.* 106:3312–24
79. Sancho-García JC, Pérez-Jiménez AJ, San-Fabián F. 2000. A comparison between DFT and other ab initio schemes on the activation energy in the automerization of cyclobutadiene. *Chem. Phys. Lett.* 317:245–51
80. Sancho-García JC, San-Fabián F. 2003. Usefulness of the Colle-Salvetti model for the treatment of the nondynamic correlation. *J. Chem. Phys.* 118:1054–58
81. Pastor-Abia L, Pérez-Jiménez A, Pérez-Jordá JM, Sancho-García JC, San-Fabián E, Moscardó F. 2003. Correlation factor approach to the correlation energy functional. *Theor. Chem. Acc.* 111:1–17
82. Malcolm NOJ, McDouall JJW. 1997. Combining multiconfigurational wave functions with density functional estimates of dynamic electron correlation. 2. Effect of improved valence correlation. *J. Phys. Chem. A* 101:8119–22
83. San-Fabián E, Pastor-Abia L. 2002. DFT calculations of correlation energies for excited electronic states using MCSCF wave functions. *Int. J. Quantum Chem.* 91:451–60
84. Takeda R, Yamanaka S, Yamaguchi K. 2002. CAS-DFT based on odd-electron density and radical density. *Chem. Phys. Lett.* 366:321–28
85. Takeda R, Yamanaka S, Yamaguchi K. 2003. Approximate on-top pair density into one-body functions for CAS-DFT. *Int. J. Quantum Chem.* 96:463–73
86. Stoll H, Pavlidou CME, Preuß H. 1980. On the calculation of correlation energies in the spin-density functional formalism. *Theor. Chim. Acta* 49:143–49
87. Staroverov VN, Davidson ER. 2000. Diradical character of the cope rearrangement transition state. *J. Am. Chem. Soc.* 122:186–87
88. Tsuchimochi T, Scuseria GE. 2009. Strong correlations via constrained-pairing mean-field theory. *J. Chem. Phys.* 131:121102
89. Tsuchimochi T, Scuseria GE, Savin A. 2009. Constrained-pairing mean-field theory. III. Inclusion of density functional exchange and correlation effects via alternative densities. *J. Chem. Phys.* 132:024111
90. Tsuchimochi T, Henderson TM, Scuseria GE, Savin A. 2010. Constrained-pairing mean-field theory. IV. Inclusion of corresponding pair constraints and connection to unrestricted Hartree-Fock theory. *J. Chem. Phys.* 133:134108
91. Ellis JK, Jiménez-Hoyos CA, Henderson TM, Tsuchimochi T, Scuseria GE. 2011. Constrained-pairing mean-field theory. V. Triplet pairing formalism. *J. Chem. Phys.* 135:034112
92. Tao J, Perdew JP, Staroverov VN, Scuseria GE. 2003. Climbing the density functional ladder: nonempirical meta-generalized gradient approximation designed for molecules and solids. *Phys. Rev. Lett.* 91:146401
93. Garza AJ, Bulik IW, Henderson TM, Scuseria GE. 2015. Synergy between pair coupled cluster doubles and pair density functional theory. *J. Chem. Phys.* 142:044109

94. Sand AM, Truhlar DG, Gagliardi L. 2017. Efficient algorithm for multiconfiguration pair-density functional theory with application to the heterolytic dissociation energy of ferrocene. *J. Chem. Phys.* 146:34101
95. Sand AM, Hoyer CE, Sharkas K, Kidder KM, Lindh R, et al. 2018. Analytic gradients for complete active space pair-density functional theory. *J. Chem. Theory Comput.* 14:126–38
96. Scott TR, Hermes MR, Sand AM, Oakley MS, Truhlar DG, Gagliardi L. 2020. Analytic gradients for state-averaged multiconfiguration pair-density functional theory. *J. Chem. Phys.* 153:014106
97. Schollwöck U. 2005. The density-matrix renormalization group. *Rev. Mod. Phys.* 77:259–315
98. Chan GKL, Zgid D. 2009. The density matrix renormalization group in quantum chemistry. *Annu. Rep. Comput. Chem.* 5:149–62
99. Keller S, Dolfi M, Troyer M, Reiher M. 2015. An efficient matrix product operator representation of the quantum chemical Hamiltonian. *J. Chem. Phys.* 143:244118
100. Knecht S, Hedegård ED, Keller S, Kovyrshin A, Ma Y, et al. 2016. New approaches for ab initio calculations of molecules with strong electron correlation. *Chimia* 70:244–51
101. DePrince AE III, Mazziotti DA. 2007. Parametric approach to variational two-electron reduced-density-matrix theory. *Phys. Rev. A* 76:42501
102. Fosso-Tande J, Nguyen T-S, Gidofalvi G, DePrince AE III. 2016. Large-scale variational two-electron reduced-density-matrix-driven complete active space self-consistent field methods. *J. Chem. Theory Comput.* 12:2260–71
103. Sharma P, Bernales V, Knecht S, Truhlar DG, Gagliardi L. 2019. Density matrix renormalization group pair-density functional theory (DMRG-PDFT): singlet-triplet gaps in polyacenes and polyacetylenes. *Chem. Sci.* 10:1716–23
104. Carlson RK, Truhlar DG, Gagliardi L. 2015. Multiconfiguration pair-density functional theory: a fully translated gradient approximation and its performance for transition metal dimers and the spectroscopy of $\text{Re}_2\text{Cl}_8^{2-}$. *J. Comput. Theor. Chem.* 11:4077–85
105. Gáspár R. 1974. Statistical exchange for electron in shell and the $X\alpha$ method. *Acta Phys. Acad. Sci. Hung.* 35:213–18
106. Vosko SH, Wilk L, Nusair M. 1980. Accurate spin-dependent electron liquid correlation energies for local spin density calculations: a critical analysis. *Can. J. Phys.* 58:1200–11
107. Becke AD. 1988. Density-functional exchange-energy approximation with correct asymptotic behavior. *Phys. Rev. A* 38:3098–100
108. Thakkar AJ, McCarthy SP. 2009. Toward improved density functionals for the correlation energy. *J. Chem. Phys.* 131:134109
109. Zhang W, Truhlar DG, Tang M. 2013. Tests of exchange-correlation functional approximations against reliable experimental data for average bond energies of 3D transition metal compounds. *J. Chem. Theory Comput.* 9:3965–77
110. Zhang Y, Yang W. 1998. Comment on “Generalized gradient approximation made simple.” *Phys. Rev. Lett.* 80:890
111. Carlson RK, Truhlar DG, Gagliardi L. 2017. On-top pair density as a measure of left–right correlation in bond breaking. *J. Phys. Chem. A* 121:5540–47
112. Werner HJ, Meyer W. 1981. A quadratically convergent MCSCF method for the simultaneous optimization of several states. *J. Chem. Phys.* 74:5794–801
113. Truhlar DG, Mead CA. 2003. The relative likelihood of encountering conical intersections and avoided intersections on the potential energy surfaces of polyatomic molecules. *Phys. Rev. A* 68:32501
114. Sand AM, Hoyer CE, Truhlar DG, Gagliardi L. 2018. State-interaction pair-density functional theory. *J. Chem. Phys.* 149:024106
115. Dong SS, Huang KB, Gagliardi L, Truhlar DG. 2019. State-interaction pair-density functional theory can accurately describe a spiro mixed valence compound. *J. Phys. Chem. A* 123:2100–6
116. Zhou C, Gagliardi L, Truhlar DG. 2019. State-interaction pair-density functional theory for locally avoided crossings of potential energy surfaces in methylamine. *Phys. Chem. Chem. Phys.* 21:13486–93
117. Bao JJ, Zhou C, Varga Z, Kanchanakungwankul S, Gagliardi L, Truhlar DG. 2020. Multi-state pair-density functional theory. *Faraday Discuss.* 224:348–72

118. Bao JJ, Zhou C, Truhlar DG. 2020. Compressed-state multi-state pair-density functional theory. *J. Chem. Theory Comput.* 16:7444–52
119. Cohen AJ, Mori-Sánchez P, Yang W. 2008. Insights into current limitations of density functional theory. *Science* 321:792–94
120. Li C, Zheng X, Su NQ, Yang W. 2018. Localized orbital scaling correction for systematic elimination of delocalization error in density functional approximations. *Natl. Sci. Rev.* 5:203–15
121. Bao JL, Wang Y, He X, Gagliardi L, Truhlar DG. 2017. Multiconfiguration pair-density functional theory is free from delocalization error. *J. Phys. Chem. Lett.* 8:5616–20
122. Bao JL, Gagliardi L, Truhlar DG. 2018. Self-interaction error in density functional theory: an appraisal. *J. Phys. Chem. Lett.* 9:2353–58
123. Sharma P, Truhlar DG, Gagliardi L. 2018. Active space dependence in multiconfiguration pair-density functional theory. *J. Chem. Theory Comput.* 14:660–69
124. Nobes RH, Pople JA, Radom L, Handy NC, Knowles PJ. 1987. Slow convergence of the Møller-Plesset perturbation series: the dissociation energy of hydrogen cyanide and the electron affinity of the cyano radical. *Chem. Phys. Lett.* 138:481–85
125. Ivanic J, Ruedenberg K. 2002. Deadwood in configuration spaces. II. Singles + doubles and singles + doubles + triples + quadruples spaces. *Theor. Chem. Acc.* 107:220–28
126. Odoh SO, Manni GL, Carlson RK, Truhlar DG, Gagliardi L. 2016. Separated-pair approximation and separated-pair pair-density functional theory. *Chem. Sci.* 7:2399–413
127. Tishchenko O, Zheng J, Truhlar DG. 2008. Multireference model chemistries for thermochemical kinetics. *J. Chem. Theory Comput.* 4:1208–19
128. Bao JL, Sand A, Gagliardi L, Truhlar DG. 2016. Correlated-participating-orbitals pair-density functional method and application to multiplet energy splittings of main-group divalent radicals. *J. Chem. Theory Comput.* 12:4274–83
129. Pople JA. 1999. Nobel lecture: quantum chemical models. *Rev. Mod. Phys.* 71:1267–74
130. Bao JJ, Dong SS, Gagliardi L, Truhlar DG. 2018. Automatic selection of an active space for calculating electronic excitation spectra by MS-CASPT2 or MC-PDFT. *J. Chem. Theory Comput.* 14:2017–25
131. Bao JJ, Truhlar DG. 2019. Automatic active space selection for calculating electronic excitation energies based on high-spin unrestricted Hartree-Fock orbitals. *J. Chem. Theory Comput.* 15:5308–18
132. Mostafanejad M, DePrince AE III. 2019. Combining pair-density functional theory and variational two-electron reduced-density matrix methods. *J. Chem. Theory Comput.* 15:290–302
133. Mostafanejad M, Liebenthal MD, DePrince AE III. 2020. Global hybrid multiconfiguration pair-density functional theory. *J. Comput. Theor. Chem.* 16:2274–83
134. Gritsenko OV, van Meer R, Pernal K. 2018. Efficient evaluation of electron correlation along the bond-dissociation coordinate in the ground and excited ionic states with dynamic correlation suppression and enhancement functions of the on-top pair density. *Phys. Rev. A* 98:062510
135. Gritsenko OV, van Meer R, Pernal K. 2018. Electron correlation energy with a combined complete active space and corrected density-functional approach in a small basis versus the reference complete basis set limit: a close agreement. *Chem. Phys. Lett.* 716:227–30
136. Gritsenko OV, Pernal K. 2019. Complete active space and corrected density functional theories helping each other to describe vertical electronic $\pi \rightarrow \pi^*$ excitations in prototype multiple-bonded molecules. *J. Chem. Phys.* 151:024111
137. Pernal K, Gritsenko OV, van Meer R. 2019. Reproducing benchmark potential energy curves of molecular bond dissociation with small complete active space aided with density and density-matrix functional corrections. *J. Chem. Phys.* 151:164122
138. Aquilante F, Autschbach J, Carlson RK, Chibotaru LF, Delcey MG, et al. 2016. Molcas 8: new capabilities for multiconfigurational quantum chemical calculations across the periodic table. *J. Comput. Chem.* 5:506–41
139. Sun Q, Berkelbach TC, Blunt NS, Booth GH, Guo S, et al. 2018. PySCF: the Python-based simulations of chemistry framework. *WIREs Comput. Mol. Sci.* 8:e1340
140. Hermes MR. 2020. MatthewRHermes GitHub repository. *GitHub*. <https://github.com/MatthewRHermes/mrh>

141. Gordon MS, Schmidt MW. 2005. Advances in electronic structure theory: GAMESS a decade later. In *Theory and Applications of Computational Chemistry*, ed. C Dykstra, G Frenking, K Kim, G Scuseria, pp. 1167–89. Amsterdam: Elsevier
142. Ghosh S, Sonnenberger AL, Hoyer CE, Truhlar DG, Gagliardi L. 2015. Multiconfiguration pair-density functional theory outperforms Kohn-Sham density functional theory and multireference perturbation theory for ground-state and excited-state charge transfer. *J. Chem. Theory Comput.* 11:3643–49
143. Bao JL, Odoh SO, Gagliardi L, Truhlar DG. 2017. Predicting bond dissociation energies of transition-metal compounds by multiconfiguration pair-density functional theory and second-order perturbation theory based on correlated participating orbitals and separated pairs. *J. Chem. Theory Comput.* 13:616–26
144. Sharkas K, Gagliardi L, Truhlar DG. 2017. Multiconfiguration pair-density functional theory and complete active space second order perturbation theory. Bond dissociation energies of FeC, NiC, FeS, NiS, FeSe, and NiSe. *J. Phys. Chem. A* 121:9392–400
145. Bao JJ, Gagliardi L, Truhlar DG. 2017. Multiconfiguration pair-density functional theory for doublet excitation energies and excited state geometries: the excited states of CN. *Phys. Chem. Chem. Phys.* 19:30089–96
146. Oakley MS, Bao JJ, Klobukowski M, Truhlar DG, Gagliardi L. 2018. Multireference methods for calculating the dissociation enthalpy of tetrahedral P₄ to two P₂. *J. Phys. Chem. A* 122:5742–49
147. Bao LJ, Verma P, Truhlar DG. 2018. How well can density functional theory and pair-density functional theory predict the correct atomic charges for dissociation and accurate dissociation energetics of ionic bonds? *Phys. Chem. Chem. Phys.* 20:23072–78
148. Bao JJ, Gagliardi L, Truhlar DG. 2019. Weak interactions in alkaline earth metal dimers by pair-density functional theory. *J. Phys. Chem. Lett.* 10:799–805
149. Roos BO, Lindh R, Malmqvist PA, Veryzaov V, Widmark PO. 2004. Main group atoms and dimers studied with a new relativistic ANO basis set. *J. Phys. Chem. A* 108:2851–58
150. Li S, Gagliardi L, Truhlar DG. 2020. Extended separated-pair approximation for transition metal potential energy curves. *J. Chem. Phys.* 152:124118
151. Zhao Y, Truhlar DG. 2006. Assessment of model chemistries for noncovalent interactions. *J. Chem. Theory Comput.* 2:1009–18
152. Carlson RK, Li Manni G, Sonnenberger AL, Truhlar DG, Gagliardi L. 2015. Multiconfiguration pair-density functional theory: barrier heights and main group and transition metal energetics. *J. Chem. Theory Comput.* 11:82–90
153. Sand AM, Kidder KM, Truhlar DG, Gagliardi L. 2019. Calculation of chemical reaction barrier heights by multiconfiguration pair-density functional theory with correlated participating orbitals. *J. Phys. Chem. A* 123:9809–17
154. Ghosh S, Cramer CJ, Truhlar DG, Gagliardi L. 2017. Generalized-active-space pair-density functional theory: an efficient method to study large, strongly correlated, conjugated systems. *Chem. Sci.* 8:2741–50
155. Wilbraham L, Verma P, Truhlar DG, Gagliardi L, Ciofini I. 2017. Multiconfiguration pair-density functional theory predicts spin-state ordering in iron complexes with the same accuracy as complete active space second-order perturbation theory at a significantly reduced computational cost. *J. Phys. Chem. Lett.* 8:2026–30
156. Stoneburner SJ, Truhlar DG, Gagliardi L. 2018. MC-PDFT can calculate singlet-triplet splittings of organic diradicals. *J. Chem. Phys.* 148:64108
157. Presti D, Stoneburner SJ, Truhlar DG, Gagliardi L. 2019. Full correlation in a multiconfigurational study of bimetallic clusters: restricted active space pair-density functional theory study of [2Fe-2S] systems. *J. Phys. Chem. C* 123:11899–907
158. Zhou C, Gagliardi L, Truhlar DG. 2019. Multiconfiguration pair-density functional theory for iron porphyrin with CAS, RAS, and DMRG active spaces. *J. Phys. Chem. A* 123:3389–94
159. Hoyer CE, Gagliardi L, Truhlar DG. 2015. Multiconfiguration pair-density functional theory spectral calculations are stable to adding diffuse basis functions. *J. Phys. Chem. Lett.* 6:4184–88
160. Hoyer CE, Ghosh S, Truhlar DG, Gagliardi L. 2016. Multiconfiguration pair-density functional theory is as accurate as CASPT2 for electronic excitation. *J. Phys. Chem. Lett.* 7:586–91

161. Dong SS, Gagliardi L, Truhlar DG. 2018. Excitation spectra of retinal by multiconfiguration pair-density functional theory. *Phys. Chem. Chem. Phys.* 20:7265–76
162. Sharma P, Bernales V, Truhlar DG, Gagliardi L. 2018. Valence $\pi\pi^*$ excitations in benzene studied by multiconfiguration pair-density functional theory. *J. Phys. Chem. Lett.* 10:75–81
163. Presti D, Truhlar DG, Gagliardi L. 2018. Intramolecular charge transfer and local excitation in organic fluorescent photoredox catalysts explained by RASCI-PDFT. *J. Phys. Chem. C* 122:12061–70
164. Dong SS, Gagliardi L, Truhlar DG. 2019. Nature of the 1^1B_u and 2^1A_g excited states of butadiene and the Goldilocks principle of basis set diffuseness. *J. Chem. Theory Comput.* 15:4591–601
165. Ning J, Truhlar DG. 2020. The valence and Rydberg states of dienes. *Phys. Chem. Chem. Phys.* 22:6176–83
166. Sharma P, Truhlar DG, Gagliardi L. 2018. Multiconfiguration pair-density functional theory investigation of the electronic spectrum of MnO_4^- . *J. Chem. Phys.* 148:124305

Contents

My Trajectory in Molecular Reaction Dynamics and Spectroscopy <i>Robert Benny Gerber</i>	1
My Life in Changing Times: New Ideas and New Techniques <i>Ruth M. Lynden-Bell</i>	35
Critical Phenomena in Plasma Membrane Organization and Function <i>Thomas R. Shaw, Subhadip Ghosh, and Sarah L. Veatch</i>	51
Droplet Interfacial Tensions and Phase Transitions Measured in Microfluidic Channels <i>Priyatanu Roy, Shibao Liu, and Cari S. Dutcher</i>	73
First-Principles Insights into Plasmon-Induced Catalysis <i>John Mark P. Martirez, Junwei Lucas Bao, and Emily A. Carter</i>	99
Optical Properties and Excited-State Dynamics of Atomically Precise Gold Nanoclusters <i>Meng Zhou and Rongchao Jin</i>	121
α -Crystallins in the Vertebrate Eye Lens: Complex Oligomers and Molecular Chaperones <i>Marc A. Sprague-Piercy, Megan A. Rocha, Ashley O. Kwok, and Rachel W. Martin</i>	143
Vibronic and Environmental Effects in Simulations of Optical Spectroscopy <i>Tim J. Zuehlsdorff, Sapana V. Shedge, Shao-Yu Lu, Hanbo Hong, Vincent P. Aguirre, Liang Shi, and Christine M. Isborn</i>	165
Molecular Simulation of Electrode-Solution Interfaces <i>Laura Scalfi, Mathieu Salanne, and Benjamin Rotenberg</i>	189
Electrochemical Tip-Enhanced Raman Spectroscopy: An In Situ Nanospectroscopy for Electrochemistry <i>Sheng-Chao Huang, Yi-Fan Bao, Si-Si Wu, Teng-Xiang Huang, Matthew M. Sartin, Xiang Wang, and Bin Ren</i>	213

Atomic Force Microscopy: An Emerging Tool in Measuring the Phase State and Surface Tension of Individual Aerosol Particles <i>Hansol D. Lee and Alexei V. Tivanski</i>	235
Cryogenic Super-Resolution Fluorescence and Electron Microscopy Correlated at the Nanoscale <i>Peter D. Dahlberg and W. E. Moerner</i>	253
Vibrational Sum-Frequency Generation Hyperspectral Microscopy for Molecular Self-Assembled Systems <i>Haoyuan Wang and Wei Xiong</i>	279
Quantitative Mass Spectrometry Imaging of Biological Systems <i>Daisy Unsibuary, Daniela Mesa Sanchez, and Julia Laskin</i>	307
In Situ Surface-Enhanced Raman Spectroscopy Characterization of Electrocatalysis with Different Nanostructures <i>Bao-Ying Wen, Qing-Qi Chen, Petar M. Radjenovic, Jin-Chao Dong, Zhong-Qun Tian, and Jian-Feng Li</i>	331
Quantum-State Control and Manipulation of Paramagnetic Molecules with Magnetic Fields <i>Brianna R. Heazlewood</i>	353
Dry Deposition of Atmospheric Aerosols: Approaches, Observations, and Mechanisms <i>Delphine K. Farmer, Erin K. Boedicker, and Holly M. DeBolt</i>	375
Spectroscopy and Scattering Studies Using Interpolated Ab Initio Potentials <i>Ernesto Quintas-Sánchez and Richard Dawes</i>	399
Control of Chemical Reaction Pathways by Light-Matter Coupling <i>Dinumol Devasia, Ankita Das, Varun Mohan, and Prashant K. Jain</i>	423
First-Principles Simulations of Biological Molecules Subjected to Ionizing Radiation <i>Karwan Ali Omar, Karim Hasnaoui, and Aurélien de la Lande</i>	445
Cascaded Biocatalysis and Bioelectrocatalysis: Overview and Recent Advances <i>Yoo Seok Lee, Koun Lim, and Shelley D. Minteer</i>	467
Multiscale Models for Light-Driven Processes <i>Michele Nottoli, Lorenzo Cupellini, Filippo Lipparini, Giovanni Granucci, and Benedetta Mennucci</i>	489
Modeling Spin-Crossover Dynamics <i>Saikat Mukherjee, Dmitry A. Fedorov, and Sergey A. Varganov</i>	515

Multiconfiguration Pair-Density Functional Theory <i>Prachi Sharma, Jie J. Bao, Donald G. Trublar, and Laura Gagliardi</i>	541
Optical Force-Induced Chemistry at Solution Surfaces <i>Hiroshi Masubara and Ken-ichi Yuyama</i>	565
Quantum Dynamics of Exciton Transport and Dissociation in Multichromophoric Systems <i>Irene Burghardt, Wjatscheslaw Popp, Dominik Brey, and Robert Binder</i>	591
Understanding and Controlling Intersystem Crossing in Molecules <i>Christel M. Marian</i>	617
From Intermolecular Interaction Energies and Observable Shifts to Component Contributions and Back Again: A Tale of Variational Energy Decomposition Analysis <i>Yuezhi Mao, Matthias Loipersberger, Paul R. Horn, Aksbaya Kumar Das, Omar Demerdash, Daniel S. Levine, Srimukh Prasad Veccham, Teresa Head-Gordon, and Martin Head-Gordon</i>	641
Demystifying the Diffuse Vibrational Spectrum of Aqueous Protons Through Cold Cluster Spectroscopy <i>Helen J. Zeng and Mark A. Johnson</i>	667

Errata

An online log of corrections to *Annual Review of Physical Chemistry* articles may be found at <http://www.annualreviews.org/errata/physchem>